

Response Improvement of Hydraulic Robotic Joints via A Force Servo and Inverted Pendulum Demo

Ryo Arai¹, Satoru Sakai¹, and Kazuki Ono¹

Abstract—In this paper, a force servo for hydraulic robot joints is designed and applied to an inverted pendulum demo. First, the nonlinear nominal model of the hydraulic cylinder is reviewed, and the nominal integrator is introduced. Second, through a partial fusion of our modeling and control techniques, a force servo is designed based on a modification of the nominal integrator as an intermediate stage. Finally, against the non-short hydraulic pipes (1.9 m), the response is improved by the designed force servo in the presence of rotational motion effects.

I. INTRODUCTION

Hydraulic arms have been used in the field of extreme environments such as construction, agriculture, and demining and so on due to their higher robustness and significantly larger power-to-weight ratio compared to electric arms. Unmanned hydraulic arms are gaining popularity, and a new generation of model based control for hydraulic arms is coming (e.g., [1], [2], [3]). In hydraulic robotics, there are two ways toward model based control. The first way, we construct a new controller using the structural properties of hydraulic robots (e.g., [4], [5]). However, controllers designed for traditional and fruitful electric robots are not applicable directly. In the second way, we construct a servo as an interface between hydraulic robots and existing (new) controllers for electric robots (e.g., [6], [7]). Once we have a good force servo, almost all existing controllers for electric robots can be applicable to hydraulic robots. This paper discusses the second way of model based control for hydraulic robotics. The driving force of a cylinder in hydraulic robotics corresponds to the driving torque in traditional electric robotics. Of course, there are many conventional (model based) force servos. For example, Semini *et al.* discuss the driving torque control [8] based on feedback linearization. Zhu and Piedboeuf discuss the adaptive output control scheme [9]. In all, to our knowledge, however, many conventional force servos as shown in Table I cancel (nominal) nonlinearity in the hydraulic cylinder dynamics in order to design a linear controller (e.g., PID controller). In terms of robust control [10] it is well known that such (nominal) nonlinearity canceling may be fragile against the uncertainty dynamics. On the other hand, even in a (almost) linear framework, a two degree-of-freedom (2DOF) control [11], [12] point of view is not fully applied as shown in Table I. As the closest report to this paper, Obara discusses a 2DOF design [13] via a set of the coordinate transformation using the Casimir functions and the Hamiltonian replacement

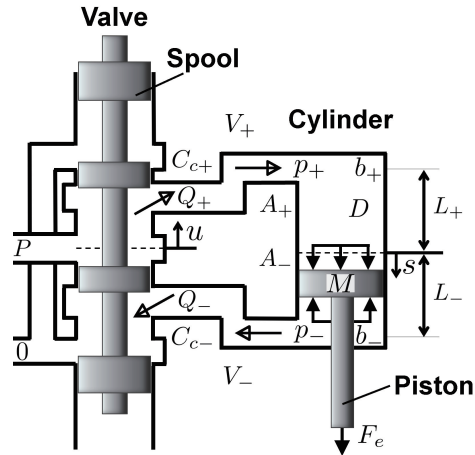


Fig. 1. A hydraulic cylinder, pipes, and a servo valve.

[14]. However, there are only numerical results and any experimental result is not discussed.

In this paper, the proposed force servo is applied to the well known inverted pendulum for improving the readability. As in a previous report, Bucher Hydraulics presents an experimental video of an inverted pendulum using a translational hydraulic actuator [15]. The details are not open but the design would use the standard control error ($r - y$) in the absence of the rotational motion effects (e.g., centrifugal force disturbance).

As a partial fusion of the two techniques: a set of the coordinate transformation using the Casimir functions and the Hamiltonian replacement [14] and a 2DOF design [11], [12], in the paper on the stair landing, a force servo controller design example using the two techniques is provided and applied to an inverted pendulum demo in the presence of rotational motion effects. Against the uncertainty dynamics, the designed controller can be robust and not fragile. Note that the linear approximation is never applied and the proposed approach is different from the feedback linearization (canceling) approach against the uncertainty.

The remaining part of the paper is organized as follows. In Section II, a review of hydraulic cylinder dynamics is provided. In Section III, a proposed force servo is designed. In Section IV, the effectiveness of the proposed force servo is confirmed and visualized experimentally by an inverted pendulum. Finally, Section VI concludes this paper.

¹Ryo Arai, Satoru Sakai, Kazuki Ono are with Faculty of Mechanical Engineering, University of Shinshu

TABLE I
CONVENTIONAL AND PROPOSED FORCE SERVO.

	(Nominal) Nonlinear canceling	Degree of freedom in controller design
Semini <i>et al.</i> [8]	YES (FB linearization)	1 (Feedback)
Zhu and Piedboeuf [9]	YES (Adaptive control)	1 (Feedback)
Proposed	NO (Automatic modification)	2 (Feedback and feedforward)

II. PRELIMINARY

In this section, we review a nonlinear nominal model of a hydraulic cylinder dynamics and a Casimir function, which is a structural property of mechanical systems that have driving systems, such as dynamic actuators or dynamic flexibility.

A. Nonlinear nominal model [16]

Fig. 1 shows a hydraulic cylinder, pipes, and a valve. We review the nominal model in the original representation [16]

$$\begin{cases} M\dot{s} &= -D\dot{s} + A_+p_+ - A_-p_- + F_e \\ \dot{p}_+ &= \frac{b_+}{V_+(s(t))}[-A_+\dot{s} + Q_+(p_+, u)] \\ \dot{p}_- &= \frac{b_-}{V_-(s(t))}[+A_-\dot{s} - Q_-(p_-, u)] \end{cases} \quad (1)$$

where the displacement $s(t)$ [m], the cap pressure $p_+(t)$ [Pa], the rod pressure $p_-(t)$ [Pa], the external force F_e [N], and the spool displacement (the input) $u(t)$ [m] are the functions of time t [s]. The subscript $+$ and $-$ denote the cap-side and the rod-side, respectively, and the subscript \pm denotes both sides. The driving force is $F(t) = A_+p_+(t) - A_-p_-(t)$ [N]. The mass M [kg], the damping constant D [Ns/m], the piston areas A_{\pm} [m²] and the bulk modulus b_{\pm} [Pa] are the positive constants. The cylinder volumes $V_+(s(t)) := V_+^{\min} + A_+(L/2 + s(t))$, $V_-(s(t)) := V_-^{\min} + A_-(L/2 - s(t))$ [m³] with the constant stroke L [m] are the functions of the displacement $s(t)$. The input flows Q_+ and Q_- [m³/s], are approximated by Bernoulli's principle

$$\begin{cases} Q_+ = B(p_+, +u)u := B_+u \\ Q_- = B(p_-, -u)u := B_-u \end{cases} \quad (2)$$

with

$$B(r, u) = \begin{cases} C_{c+}\sqrt{-r+P} & (u > 0) \\ 0 & (u = 0) \\ C_{c-}\sqrt{+r-0} & (u < 0) \end{cases} \quad (3)$$

where the flow gain $C_{c\pm}$ [m/(s·√Pa)] and the source pressure P [Pa] are the positive constants. The nominal model introduces the restricted domain $s \in (-L_-, L_+)$ and $p_{\pm} \in [0, P]$ and the absolute notation within the square root functions (3) is dropped. Fig. 2 shows an example of the accuracy of the nominal model (1), (2).

B. Casimir functions [14]

Consider the system in a physical form (1) [4]. Then there exists a set of a coordinate transformation, an input transformation $v = g_f u$, and a Hamiltonian replacement which reduces the system (1) into the following system [14]

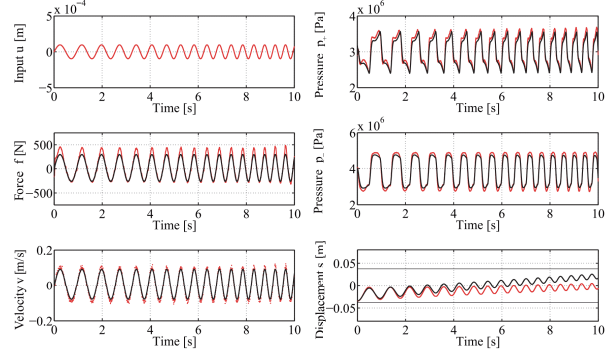


Fig. 2. Example of the nominal model output (the black curves) and the experimental output (the red dots) [16].

$$\begin{cases} \dot{x}_c = \begin{bmatrix} 0 & +I & 0 \\ -I & -D & 0 \\ 0 & 0 & 0 \end{bmatrix} \nabla_{x_c} H_{\text{simple}} + \underbrace{\begin{bmatrix} 0 \\ 0 \\ 1 \end{bmatrix}}_{g_c} v \\ y = g_c^T \nabla_{x_c} H \end{cases} \quad (4)$$

with the state $x_c := (s, p, C_f)$,

$$C_f = \int k(s) + F, \quad (5)$$

$$g_f = b_+A_+B_+V_+^{-1} + b_-A_-B_-V_-^{-1} \quad (6)$$

and the Hamiltonian function with $k(s) := \frac{b_+A_+^2}{V_+(s)} + \frac{b_-A_-^2}{V_-(s)}$

$$H_{\text{simple}} = T + \iint k(s) - sC_f. \quad (7)$$

See details [14]. Here, the nominal integrator [17], [18] $C_f = \frac{1}{s}v$ can be confirmed as a property of the nonlinear nominal model of hydraulic cylinder dynamics.

III. A FORCE SERVO DESIGN

As a partial fusion of the two techniques: a set of the coordinate transformation using the Casimir and the Hamiltonian replacement [14] and a 2DOF design [11], [12], in the paper on the stair landing (intermediate stage), a controller design example using the two techniques (our modeling and control techniques) is provided. Note that the linear approximation is never applied and the proposed approach is different from the feedback linearization (canceling) approach against the uncertainty factor.

Fig. 3 shows the signal flow. In the left top block (number one) in Fig. 3, a typical conventional force servo uses the standard control error $r - y$ in the design procedure. In the

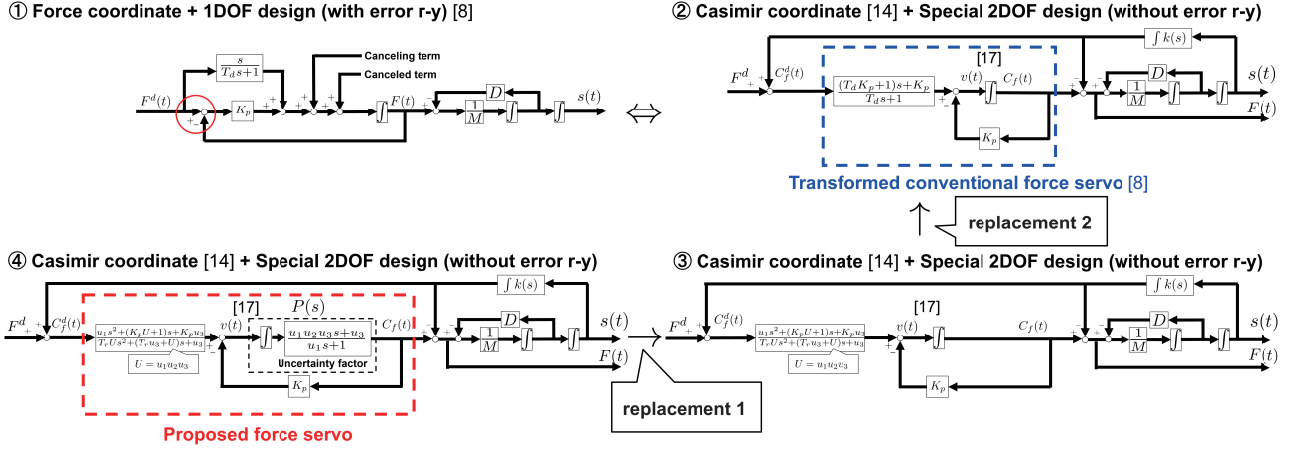


Fig. 3. Block diagram of the control system for the conventional and proposed methods. The definition of the replacement 1 is $\frac{u_1 u_2 u_3 s + u_3}{u_1 s + 1} \rightarrow 1$ and the definition of the replacement 2 is $\frac{u_1 s^2 + (K_p u_1 u_2 u_3 + 1)s + K_p u_3}{T_r u_1 u_2 u_3 s^2 + (T_r u_3 + u_1 u_2 u_3)s + u_3} \rightarrow \frac{(T_d K_p + 1)s + K_p}{T_d s + 1}$.

absence of uncertainty, the canceling term works as expected so that the (almost) linear framework is not destroyed. In the right top (number two) in Fig. 3, via a set of the coordinate transformation and the Hamiltonian replacement, the nominal integrator is rewritten and the conventional force servo is also rewritten in the pure feedback and pure feedforward form. Note that the standard control error $r - y$ does not appear any more even though the above two signal flows are equivalent to each other. This implies the corresponding signal flow of the conventional force servo ($K(r - y)$) is just a special case of a 2DOF [11], [12] signal flow ($F_F r - F_B y$) using the pure feedback ($F_F r$) and feedforward ($-F_B y$) in the presence of an additional constraint ($F_F = F_B = K$). For example, the corresponding signal flow of the conventional force servo can be generalized if a more general feedforward as shown in the right bottom (number three) is designed. The proposed force servo performance should be better than the conventional one, or should be equal to the conventional one.

Unlike the nominal model, an actual experimental setup cannot achieve the expected performance due to uncertainty such as parameter identification errors and unmodeled dynamics and so on. In an intermediate stage, in the paper, we modify the nominal integrator as [19]:

$$P(s) = \frac{N_p(s)}{D_p(s)} = \underbrace{\frac{1}{s}}_{\text{nominal integrator [17][18]}} \underbrace{\frac{u_1 u_2 u_3 s + u_3}{u_1 s + 1}}_{\text{uncertainty factor [19]}} \quad (8)$$

in which a part of uncertainty is counted as the uncertainty factor where $u_1 > 0$, $1 > u_2 > 0$, and $u_3 > 0$ are the positive constants, and can be expressed in the coprime factorization form using a set of the corresponding proper (causal) and stable transfer functions $N_p(s)$ and $D_p(s)$ using $\alpha = \frac{1 + \sqrt{1 - u_2}}{u_1 u_2} > 0$:

$$N_p(s) = \frac{u_1 u_2 u_3 s + u_3}{(s + \alpha)^2}, D_p(s) = \frac{u_1 s^2 + s}{(s + \alpha)^2}. \quad (9)$$

Then a set of the pure feedback $F_B(s)$ and feedforward

$F_F(s)$ that achieves the internal stability are always represented as follows:

$$F_B(s) = \frac{N_s + Q(s)D_p(s)}{D_s - Q(s)N_p(s)}, F_F(s) = \frac{R(s)}{D_s - Q(s)N_p(s)} \quad (10)$$

where the proper and stable transfer functions N_s and D_s :

$$N_s = \alpha^2 u_3^{-1}, D_s = u_1^{-1} \quad (11)$$

are the special solution of the Bezout equation:

$$N_p(s)N_s + D_p(s)D_s = 1 \quad (12)$$

and the proper and stable transfer functions $Q(s)$ and $R(s)$ as free parameters are designed as:

$$Q(s) = \frac{Q_2 s^2 + Q_1 s + Q_0}{u_1^5 u_2^4 u_3 s^2 + (K_p u_1^5 u_2^5 u_3^2 + u_1^4 u_2^4 u_3) s + K_p u_1^4 u_2^4 u_3^2} \quad (13)$$

$$Q_2 = u_1^2 u_2^2 (u_2 - 2 - 2\sqrt{1 - u_2} + K_p u_1 u_2^2 u_3)$$

$$Q_1 = 2u_1 u_2 (3u_2 - 4 + K_p u_1 u_2^2 u_3 + \sqrt{1 - u_2} (u_2 - 4 + K_p u_1^2 u_2^3 u_3))$$

$$Q_0 = 8u_2 - u_2^2 - 8 + \sqrt{1 - u_2} (2u_2 - 6) - 2(1 - u_2)^{3/2} + K_p u_1 u_2^2 u_3 (2 + 2\sqrt{1 - u_2} - u_2)$$

$$R(s) = \frac{u_1^2 u_2^2 s^2 + 2u_1 u_2 (1 + \sqrt{1 - u_2}) s + 2 - 2\sqrt{1 - u_2} - u_2}{u_1^3 u_2^3 T_r s^2 + (u_1^3 u_2^3 u_3 + u_1^2 u_2^3 u_3 T_r) s + u_1^2 u_2^3 u_3} \quad (14)$$

with the time constant T_r ($C_f/C_f^d = 1/(T_r s + 1)$) and the feedback gain K_p are the positive constant as shown in the left bottom (number four) in Fig. 3 as an intermediate stage.

Note that by replacing the uncertainty factor with unity (replacement 1) and also specialization (replacement 2), the designed feedback and feedforward provide the conventional force servo:

$$\dot{F} = \dot{F}^d + K_p (F^d - F) \quad (15)$$

where the time derivative is implemented via the pseudo time derivative $\frac{s}{T_d s + 1}$ (LPF + pure derivative) with the time constant T_d as shown in Fig. 3.

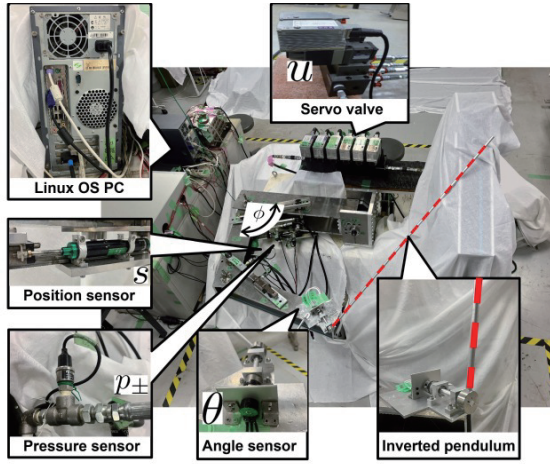


Fig. 4. The experimental setup with the non-short hydraulic pipes (1.9 m).

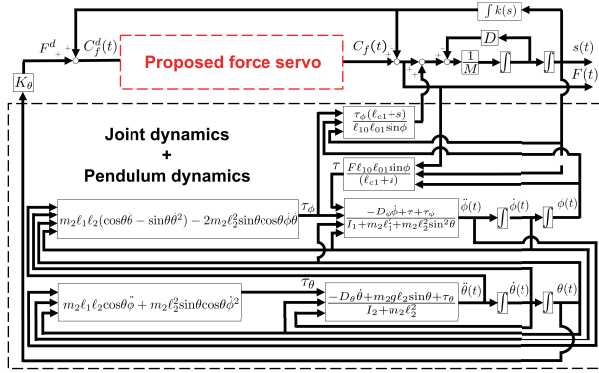


Fig. 5. The system configuration with the inverted pendulum.

IV. EXPERIMENT

In this section, we apply a force servo controller design example to an inverted pendulum demo in the presence of rotational motion effects (e.g., centrifugal force disturbance). No order made cylinders, valves, pipes are used in our experiments.

A. Conditions

Fig. 4 shows an appearance of the experimental setup. The details are exactly given in the previous paper [20]. Fig. 5 shows the system configuration with the inverted pendulum. This system has the pendulum angle θ , the hydraulic robotic joint angle ϕ , the pendulum mass m_2 , the distance between the joint center and the tip of the hydraulic robotic joint l_1 , the distance between the pendulum joint center and the center of the gravity l_2 , the moment of inertia of the hydraulic robotic joint I_1 , and the moment of inertia of the pendulum I_2 . The details of l_{c1} , l_{o1} , and l_{o2} are exactly given in the previous paper [20]. In the paper, we assume that the driving force is the force $A_+p_+ - A_-p_-$ obtained from the pressure measurement without using a force sensor while neglecting the effect of any frictional force. The relationship between the desired driving force F^d [N] and the angle θ [deg] of the inverted pendulum is expressed by $F^d = K_\theta\theta$ where

the gain K_θ . Table II shows the value of the parameters. The physical parameters (asymmetric bulk modulus $b_+ \neq b_-$ and flow gains $C_{c\pm}$) and uncertainty gains u_1 , u_2 , and u_3 are identified based on a slight extension of the existing parameter identification method [19]. Note that the identified bulk modulus are smaller than that of the hydraulic oil alone because the hydraulic pipes are made of rubber.

TABLE II
THE PHYSICAL PARAMETERS.

Symbol	Parameter	Value	Unit
L_{\pm}	Cap and Rod strokes	3.8×10^{-2}	m
A_+	Cap area	7.0×10^{-4}	m ²
A_-	Rod area	5.4×10^{-4}	m ²
V_{\pm}^{\min}	Pipe volumes	5.9×10^{-5}	m ³
b_+	Cap bulk modulus	1.4×10^8	Pa
b_-	Rod bulk modulus	1.2×10^8	Pa
C_{c+}	Cap flow gain	2.8×10^{-4}	m/(s√Pa)
C_{c-}	Rod flow gain	2.7×10^{-4}	m/(s√Pa)
P	Source pressure	7.0×10^6	Pa
u_1	Uncertainty gain	2.7×10^{-3}	—
u_2	Uncertainty gain	2.9×10^{-2}	—
u_3	Uncertainty gain	1.3	—
I_2	Moment of inertia	1.8×10^{-4}	kg·m ²
m_2	Mass of pendulum	2.1×10^{-1}	kg
l_2	Length of pendulum	0.5	m

B. Results

Fig. 6 shows the time responses of the spool displacement u [m], the driving force F [N], and the pendulum angle θ [deg]. The red plot denotes the proposed force servo and the blue plot denotes the conventional one. Fig. 7 shows the photographs of the inverted pendulum during the experiment. In the proposed force servo, the inverted pendulum oscillated three times and balanced at time $t = 1.5$ [s]. In the conventional force servo, the inverted pendulum was not balanced. Fig. 8 shows the time responses of the spool displacement u [m] as the input and the driving force F [N] for the proposed and conventional servos in the step response experiment. In the proposed force servo, the relative steady state error was 0.056 N (the desired: 500 N, the absolute error 28 N). In the conventional force servo, the relative steady state error was 0.46 N (the desired: 500 N, the absolute error 230 N). Fig. 9 shows the trajectories of the piston velocity \dot{s} , the pendulum angle θ and the pendulum angular velocity $\dot{\theta}$ corresponding to Fig. 7. In case of the proposed force servo, the origin in the three dimensional space is asymptotically stable.

C. Discussion

Figs. 6, 8, and 9 imply that the response is improved by the proposed force servo in the presence of rotational motion effects (e.g., centrifugal force disturbance) and the additional effects (e.g., mechanical friction, flexibility, and gravity disturbances). Remarkably, the response improvement is achieved against the non-short hydraulic pipes (1.9 m) in the experimental setup. In the sense that the uncertainty factor and the free parameter setting are still restrictive, the paper is just on the stair landing (intermediate stage) and the further response improvement will be reported.

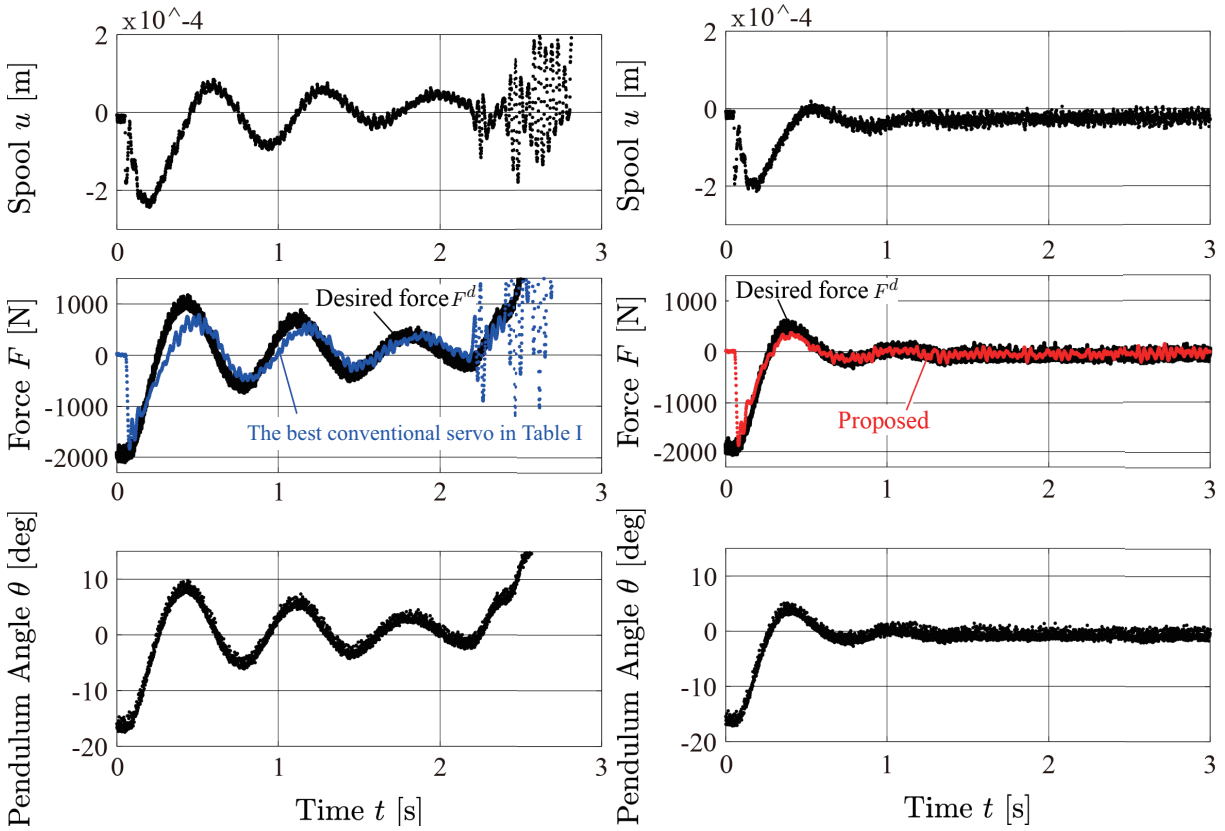


Fig. 6. Time responses of the spool displacement u , the driving force F , and the pendulum angle θ . The control starts at $t = 0.1$ [s].

The best conventional servo in Table I $\theta(0) = -16$ [deg], $\dot{\theta}(0) = 0$ [deg/s], $p_+(0) = 2.9 \times 10^6$ [Pa], $p_-(0) = 3.7 \times 10^6$ [Pa]

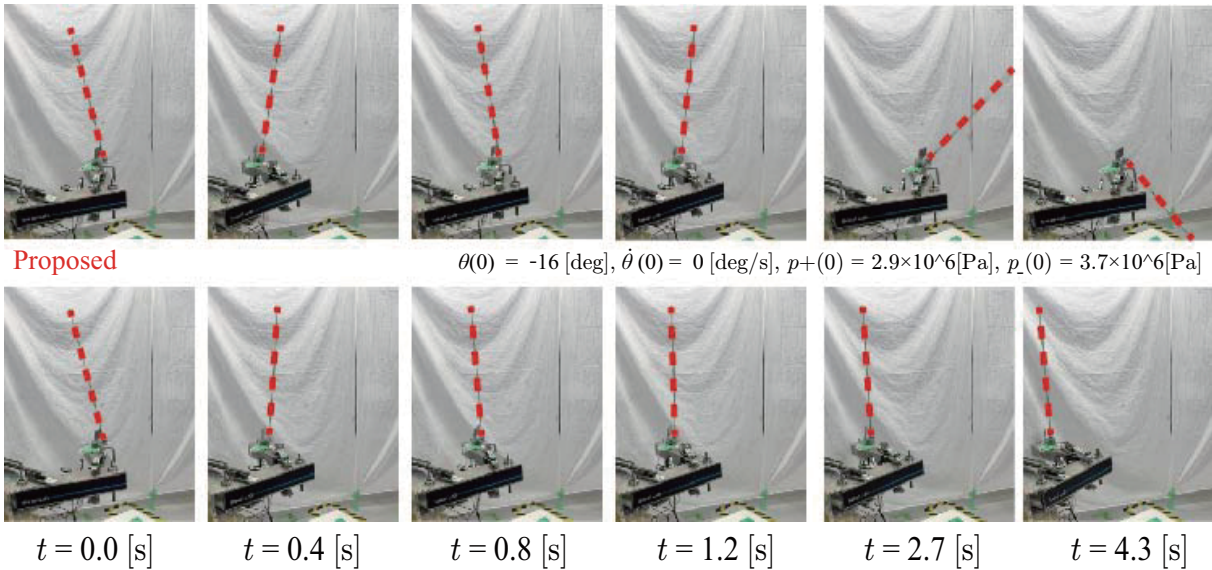


Fig. 7. The photographs of the inverted pendulum during the experiment.

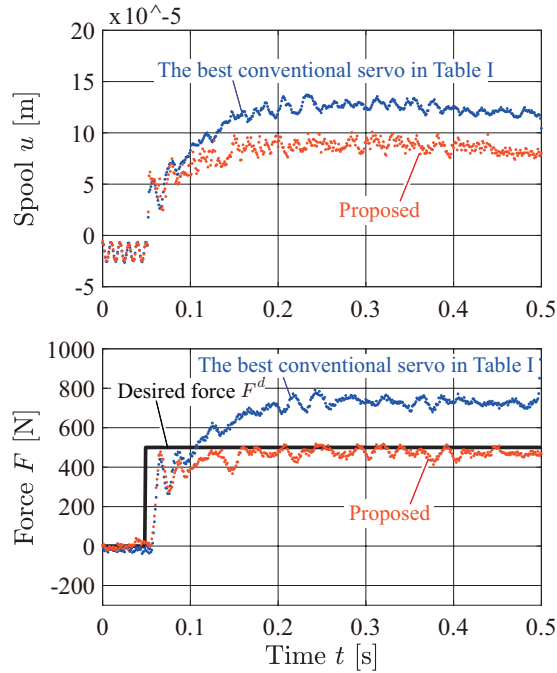


Fig. 8. Time responses of conventional and proposed driving force. The control starts at $t = 0.1$ [s].

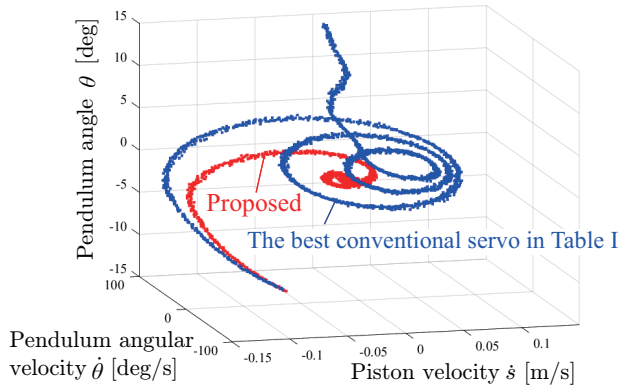


Fig. 9. The trajectories of the piston velocity \dot{s} , the pendulum angle θ , and the pendulum angular velocity $\dot{\theta}$ in the experiment of the inverted pendulum.

V. CONCLUSIONS

In this paper, a force servo for hydraulic robotic joints is designed and applied to an inverted pendulum demo in the presence of rotational motion effects. No order made cylinders, valves, pipes are used in our experiments. The response is improved by independent feedforward and feedback design procedures, which do not design the standard error $r - y$ of the conventional (model based) force servo. Note that the linear approximation is never applied and the proposed approach is different from the feedback linearization (canceling) approach against the uncertainty factor. It is impossible to capture all uncertainties. However, replacing the plant with the more uncertainty factor is also effective in improving the force response. Remarkably, the response improvement is achieved against the non-short hydraulic pipes (1.9 m) in the experimental setup. As a partial fusion of the two

techniques: a set of the coordinate transformation using the Casimir functions and the Hamiltonian replacement [14] and a 2DOF design [11], [12], a force servo design example is provided in the paper on the intermediate stage. The response is improved by the proposed force servo in the presence of rotational motion effects and so on. In the sense that the uncertainty factor and the free parameter setting are still restrictive, the paper is just on the intermediate stage, and the further response improvement will be reported.

REFERENCES

- [1] J. Mattila, J. Koivumaki, D. G. Caldwell, and C. Semini, "A survey on control of hydraulic robotic manipulators with projection to future trends," *IEEE/ASME Transactions on Mechatronics*, vol. 22, no. 2, pp. 669–680, 2017.
- [2] S. Liu, H. Chai, R. Song, Y. Li, Y. Li, Q. Zhang, P. Fu, J. Liu, and Z. Yang, "Contact force/motion hybrid control for a hydraulic legged mobile manipulator via a force-controlled floating base," *IEEE/ASME Transactions on Mechatronics*, vol. 29, no. 3, pp. 2316–2326, 2024.
- [3] Y. Xia, M. Qi, L. Lyu, Z. Jin, L. Zhang, Z. Chen, and B. Yao, "Advanced motion control of hydraulic manipulator with precise compensation of dynamic friction," *IEEE Transactions on Industrial Informatics*, vol. 20, no. 7, pp. 9375–9384, 2024.
- [4] A. Kugi and W. Kemmetmuller, "New energy-based nonlinear controller for hydraulic piston actuators," *European Journal of Control*, vol. 10, no. 2, pp. 163–173, 2004.
- [5] J. Koivumaki and J. Mattila, "Stability-guaranteed force-sensorless contact force/motion control of heavy-duty hydraulic manipulators," *IEEE Transactions on Robotics*, vol. 31, no. 4, pp. 918–935, 2015.
- [6] B. Siciliano and O. Khatib, *Springer Handbook of Robotics*. Springer-Verlag, 2007.
- [7] J.-J. E. Slotine and W. Li, *Applied Nonlinear Control*. Prentice-Hall, 1991.
- [8] C. Semini, V. Barasuol, T. Boaventura, M. Frigerio, M. Focchi, D. G. Caldwell, and J. Buchli, "Towards versatile legged robots through active impedance control," *The International Journal of Robotics Research*, vol. 34, no. 7, pp. 1003–1020, 2015.
- [9] W. H. Zhu and J. C. Piedboeuf, "Adaptive output force tracking control of hydraulic cylinders with applications to robot manipulators," *ASME Journal of Dynamic systems, Measurement and Control*, vol. 127, no. 1, pp. 206–217, 2005.
- [10] K. Zhou, J. C. Doyle, and K. Glover, *Robust and optimal control*. Prentice-Hall, 1996.
- [11] T. Sugie and T. Yoshikawa, "General solution of robust tracking problem in two-degree-of-freedom control systems," *IEEE Transactions on Automatic Control*, vol. 31, no. 6, pp. 552–554, 1986.
- [12] H. Maeda and T. Sugie, *System Control Theory for Advanced Control*. Asakura, 1990(In Japanese).
- [13] M. Obara, "Robustness improvement of the casimir based force control for nonlinear hydraulic arms," *Master Thesis* (unpublished), Shinshu University, 2021.
- [14] S. Sakai, "Fast computation by simplification of a class of hydro-mechanical system," in *Proc. of IFAC Lagrangian and Hamiltonian method for Nonlinear control*, pp. 7–12, 2012.
- [15] Bucher hydraulics, "Axial Piston Pumps AX," <https://www.bucherhydraulics.com/>, 2020.
- [16] S. Sakai and S. Stramigioli, "Visualization of hydraulic cylinder dynamics by a structure preserving nondimensionalization," *IEEE/ASME Transactions on Mechatronics*, vol. 23, no. 5, pp. 2196–2206, 2018.
- [17] S. Sakai, "Further result on the fast computation of a class of hydro-mechanical systems," in *Proc. of IFAC Lagrangian and Hamiltonian Methods for Nonlinear Control*, vol. 51, no. 3, pp. 74–79, 2018.
- [18] S. Sakai, M. Obara, and K. Chikazawa, "Parameter identification via nominal integrator of hydraulic cylinder dynamics," in *Proc. of IFAC Modelling, Identification and Control of Nonlinear Systems*, vol. 54, no. 14, pp. 78–83, 2021.
- [19] R. Arai, S. Sakai, Y. Zhang, and K. Kumabe, "Modeling improvement for hydraulic force servo via nominal integrator," in *Proc. of JFPS International Symposium on Fluid Power*, 2024(Accepted).
- [20] S. Sakai and Y. Maeshima, "A new method for parameter identification for n-dof hydraulic robots," in *Proc. of IEEE ICRA*, pp. 5983–5989, 2014.